Calcium-Mediated Fulvene Couplings. 2. Survey of 6-Aryl- and 6-Alkylfulvenes for Their *rac* Selectivity in the Synthesis of *ansa*-Calcocenes

Piet-Jan Sinnema, Britta Höhn, Robert L. Hubbard, Pamela J. Shapiro,* Brendan Twamley, Alexander Blumenfeld, and Ashwani Vij

Department of Chemistry, University of Idaho, Moscow, Idaho 83844-2343

Received July 9, 2001

The reductive coupling of 6-mesitylfulvene, 6-(3,5-di-*tert*-butylphenyl)fulvene, 6-(1-naphthyl)fulvene, and 6-*tert*-butylfulvene with $HgCl_2$-activated calcium was examined to determine if increasing the steric bulk of the 6-substituent on the fulvene would enhance selectivity for the *rac ansa*-calcocene product over the *meso* isomer. Upon formation, 6-mesitylfulvene readily dimerizes by a Diels−Alder cyclization to form (*E*,*E*)-5,10-bis(mesitylmethylene)-tricyclo[5.2.1.0]deca-3,8-diene (**1**), the X-ray crystal structure of which was determined. This fulvene does not react with activated calcium. The other fulvenes are successfully coupled by calcium; however, they afford poor to no selectivity for the *rac*-calcocene isomers in comparison with less sterically hindered 6-phenylfulvene. A 1:1 ratio of the *rac* and *meso* isomers of $\{1,1'\text{-}(1,2\text{-}t\text{-}Bu\text{-}C_2H_2)(\eta^5\text{-}C_5H_5)\}_2Ca$ (*rac*-**5** and *meso*-**5**) was obtained from the coupling of 6-*tert*-butylfulvene with calcium. The two isomers were separated by selective crystallization, and the X-ray crystal structures of the DME adducts of each isomer were determined. The crystal of *rac*-**5** contained two unique molecules of the complex. One molecule contains a single dicoordinated DME on the calcium. The other molecule contains two DME molecules: one dicoordinated and the other monocoordinated to the calcium. A variable-temperature ^{1}H NMR study of *meso*-**5** was performed to characterize two concurrent dynamic processes in the molecule. One process involves a rearrangement of the chelating ligand framework between λ and δ conformations. The other involves restricted rotations of the *tert*-butyl groups in the ethylene bridge.

The reductive coupling of fulvenes is a convenient method for generating ethylene-bridged dicyclopentadienyl ligand frameworks for *ansa*-metallocene complexes. In 1983, Brintzinger and co-workers reported the reductive coupling of 6,6-dimethylfulvene with magnesium metal to form the di Grignard reagent of the bridged ligand,[1] which has been used to prepare a variety of early-transition-metal *ansa*-metallocene complexes.[2−4] In 1991, Recknagel and Edelmann reported the one-step synthesis of *ansa*-metallocene complexes of samarium and ytterbium by the reductive coupling of 6,6-dimethylfulvene with $HgCl_2$-activated forms of the metals.[5,6] Shortly thereafter, Edelmann's group demonstrated the synthesis of *ansa*-metallocenes of calcium and strontium using this chemistry.[7]

Since we found that the *ansa*-calcocene compounds are convenient reagents for the preparation of *ansa*-metallocene complexes of chromium and other transition metals,[8−10] we have explored the calcium-mediated reductive coupling of a variety of fulvene substrates in order to determine the scope and limitations of this chemistry. One drawback to using 6,6-dimethylfulvene (and other fulvenes with reactive C−H bonds β to carbon 6) in these coupling reactions is the occurrence of unbridged ligand side products.[11] The side products arise from either hydrogen atom or proton abstraction from the neutral fulvene by the reduced fulvene radical anion or the over-reduced fulvene dianion. To avoid this problem, we employed 6-arylfulvenes in the reductive coupling reaction with activated calcium.[8] The 6-arylfulvenes are not susceptible to these side reactions; however, they afford a mixture of *rac* and *meso* calcocene isomers due to the possibility of either a *trans* or *cis* arrangement of the arene substituents in the bridge (eq 1). Fortunately, the coupling reaction exhibits a 70:30 selectivity in favor of the *rac* isomers, which are readily purified from the *meso* isomers by crystallization. Eisch and co-workers have also reported the reductive cou-

(1) Schwemlein, H.; Brintzinger, H. H. *J. Organomet. Chem.* **1983**, *254*, 69−73.
(2) Schwemlein, H.; Zsolnai, L.; Huttner, G.; Brintzinger, H. H. *J. Organomet. Chem.* **1983**, *256*, 285−289.
(3) Dorer, G.; Diebold, J.; Weyand, O.; Brintzinger, H. H. *J. Organomet. Chem.* **1992**, *427*, 245−255.
(4) Dorer, B.; Prosenc, M.-H.; Rief, U.; Brintzinger, H.-H. *Collect. Czech. Chem. Commun.* **1997**, *62*, 265−278.
(5) Recknagel, A.; Edelmann, F. T. *Angew. Chem., Int. Ed. Engl.* **1991**, *30*, 693−694.
(6) Edelmann, F. T.; Rieckhoff, M.; Haiduc, I.; Silaghi-Dumitrescu, I. *J. Organomet. Chem.* **1993**, *447*, 203−208.
(7) Rieckhoff, M.; Pieper, U.; Stalke, D.; Edelmann, F. T. *Angew. Chem., Int. Ed. Engl.* **1993**, *32*, 1079−1081.
(8) Kane, K. M.; Shapiro, P. J.; Cubbon, R.; Vij, A.; Rheingold, A. L. *Organometallics* **1997**, *16*, 4567−4571.
(9) Shapiro, P. J.; Kane, K. M.; Vij, A.; Stelck, D.; Matare, G. J.; Hubbard, R. L.; Caron, B. *Organometallics* **1999**, *18*, 3466−3473.
(10) Matare, G. J.; Foo, D. M.; Kane, K. M.; Zehnder, R.; Wagener, M.; Shapiro, P. J. *Organometallics* **2000**, *19*, 1534−1539.
(11) Sinnema, P.-J.; Shapiro, P. J.; Höhn, B.; Bitterwolf, T. E.; Twamley, B. *Organometallics* **2001**, *20*, 2883−2888.

10.1021/om010614s CCC: $22.00
Publication on Web 12/11/2001

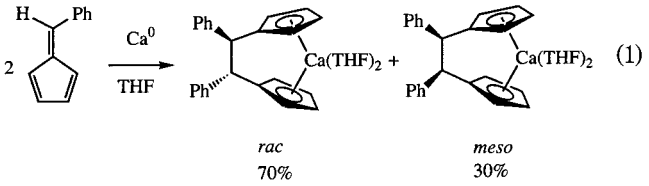

(1)

pling of 6-arylfulvenes, using divalent group 4 metal halides as the reducing agents to form group 4 *ansa*-metallocenes. They were able to improve the *rac* selectivity of the coupling reactions by increasing the size of the 6-aryl substituent on the fulvene from phenyl to 1-naphthyl to 9-anthryl.[12]

In an effort to improve the *rac* selectivity of the calcium-mediated coupling of asymmetrically substituted fulvenes, we have explored the effect of introducing bulkier groups at the 6-position of the fulvene on the stereochemical outcome of the reaction. Our results with 6-mesitylfulvene, 6-(3,5-di-*tert*-buylphenyl)fulvene, 6-(1-naphthyl)fulvene, and 6-*tert*-butylfulvene are described herein.

Results

We found in our earlier work that there is no improvement in stereoselectivity for the *rac ansa*-calcocene isomer upon replacing the phenyl substituent with a 3,4-dimethoxyphenyl substituent in the calcium-mediated reductive coupling of these 6-arylfulvenes.[10] Due to the ability of the arene ring to adopt an orientation which directs the 3,4-methoxy substituents away from the reaction site, thereby mitigating their stereodirecting effect, we decided to explore the effect of bilaterally substituted aryl groups, i.e., 6-mesitylfulvene and 6-(3,5-di-*tert*-butylphenyl)fulvene, on the stereochemical outcome of the coupling reaction.

6-Mesitylfulvene. 6-Mesitylfulvene, after preparation according to the method of Little and Stone,[13] readily forms a Diels−Alder dimer, even when diluted with petroleum ether and stored at 0 °C. A single diastereomer, the *E*,*E*-*endo* isomer, is observed in the room-temperature ^{1}H NMR spectrum of the material. The structure of the dimer, **1**, was verified by an X-ray structure determination. An ORTEP drawing of the molecule is shown in Figure 1. Crystallographic data and selected bond lengths and angles are listed in Tables 1 and 2, respectively.

The C−C bond lengths are consistent with double bonds being located at C(17)−C(27) (1.309 Å), C(19)−C(20) (1.332(6) Å), C(12)−C(13) (1.328(5) Å), and C(7)−C(11) (1.340(5) Å). The C−C single bonds within each arene ring are slightly longer, ranging from 1.372(6) to 1.406(6) Å. The single bonds C(14)−C(18) (1.567(5) Å), C(14)−C(15) (1.564(5) Å), and C(15)−C(16) (1.558 Å) at the juncture between the two fulvene rings are substantially longer than the other single C−C bonds within the dimer, reflecting the ring strain among those bridgehead carbons. The arene rings avoid steric crowding between their *o*-methyl substituents and the benzylidene hydrogen atoms by twisting out of conjugation with the exocyclic C=C bonds by 65.1° for C(22)−C(21)−C(27)−C(17) and by 69.1° for C(2)−C(1)−C(7)−C(11).

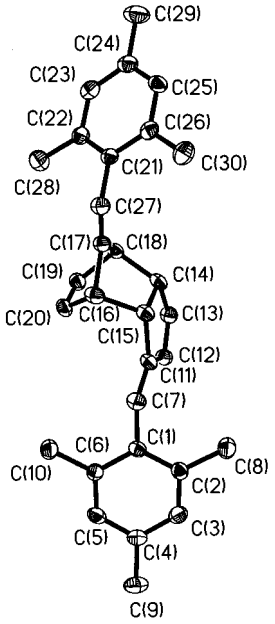

Figure 1. ORTEP drawing of **1**. The carbon atoms are shown with ellipsoids at 30% probability.

The formation of a single isomer, (*E*,*E*)-5,10-bis(mesitylmethylene)tricyclo[5.2.1.0]deca-3,8-diene, from a total of eight possible diastereomers (excluding reactions at the exocyclic double bond of the fulvene) can be rationalized from steric effects alone.[14] Whereas *exo* products are frequently observed in Diels−Alder reactions between fulvenes and other dienophiles, in this case and the other documented examples of [4 + 2] fulvene dimerization, their formation is prohibited sterically. The preferred isomer separates the bulky mesityl groups as far apart in space as possible. Upon standing, this fulvene product forms crystals of the dimer shown in Figure 1. The dimer can be cracked by heating it to 136 °C, whereupon the monomer distills over at 55 °C (20 mTorr). Reports of fulvene dimers are few,[15−17] and we are aware of no other crystallographically characterized examples. In the case of 6-(benzoyloxy)-6-phenylfulvene, only a single *endo* isomer of the dimer was detected.[15] 6,6-Bis(trifluoromethyl)fulvene also forms the endo [4 + 2] dimer selectively.[16]

Our efforts to couple the 6-mesityl fulvene monomer, even with a more active form of finely divided calcium,[18] were unsuccessful, presumably due to the tendency of the fulvene to dimerize before it can react with the calcium. Therefore, we examined a different bilaterally substituted 6-arylfulvene, 6-(3,5-di-*tert*-butylphenyl)-fulvene, which is more stable against dimerization.

6-(3,5-Di-*tert*-butylphenyl)fulvene. The reductive coupling of 6-(3,5-di-*tert*-butylphenyl)fulvene (**2**) by activated calcium was achieved by heating the reaction mixture in either refluxing THF or refluxing DME. Surprisingly, selectivity for the *rac* product with this bulky 6-arylfulvene was poor. A 1.2:1 ratio of the

(12) Eisch, J. J.; Shi, X.; Owuor, F. A. *Organometallics* **1998**, *17*, 5219−5221.
(13) Stone, K. J.; Little, R. D. *J. Org. Chem.* **1984**, *49*, 1849−1853.
(14) Fox, M. A.; Cardona, R.; Kiwiet, N. J. *J. Org. Chem.* **1987**, *52*, 1469−1474.
(15) Wennerstrom, O. *Acta Chem. Scand.* **1977**, *B31*, 915−916.
(16) Lantseva, L. T.; Martynov, B. I.; Mysov, E. I.; Dyatkin, B. L. *Zh. Org. Khim.* **1976**, *12*, 348−352.
(17) Uebersax, B.; Neuenschwander, M.; Engel, P. *Helv. Chem. Acta* **1982**, *65*, 89−104.
(18) McCormick, M. J.; Moon, K. B.; Jones, S. R.; Hanusa, T. P. *J. Chem. Soc., Chem. Commun.* **1990**, 778−779.

Table 1. Crystallographic Data for 1, *rac*-5, and *meso*-5

	1	*rac*-**5**	*meso*-**5**
empirical formula	$C_{30}H_{32}$	$C_{52}H_{86}Ca_2O_6$	$C_{24}H_{38}CaO_2$
fw	392.56	492.69	398.62
cryst syst	triclinic	orthorhombic	orthorhombic
space group	$P\bar{1}$	*Pbca*	*Pbca*
a, Å	8.6485(17)	14.3595(3)	14.9434(17)
b, Å	11.909(3)	15.7747(1)	12.5281(15)
c, Å	12.042(3)	23.8784(6)	24.351(3)
α, deg	96.95(3)	90	90
β, deg	92.62(3)	90	90
γ, deg	110.69(2)	90	90
V, Å^3	1146.4(5)	5197(5)	4558.7(9)
Z	2	4	8
T (K)	213(2)	203(2)	203(2)
λ (Å)	Mo Kα (0.710 73)	Mo Kα (0.710 73)	Mo Kα (0.710 73)
ρ_{calcd} (Mg/m^3)	1.137	1.134	1.162
μ (mm^{-1})	0.064	0.264	0.290
F(000)	424	1944	1744
cryst size (mm^3)	0.30 × 0.15 × 0.05	0.46 × 0.17 × 0.13	0.33 × 0.30 × 0.13
θ range (deg) for collected data	1.85−23.32	1.90−25.00	2.16−25
hkl limits	−9 to +9; −13 to +13;−9 to +13	−24 to +23;−12 to +12;−28 to +28	−17 to +17;−14 to +14;−18 to +28
no. of rflns collected	4470	38 196	34 253
no. of indep rflns	2997 (*R*(int) = 0.0466)	9107 (*R*(int) = 0.1027)	4008 (*R*(int) = 0.0632)
no. of data/restraints/params	2997/0/278	9107/0/575	4008/1/260
goodness of fit	1.186	0.994	1.038
R1[a]	0.0678	0.0639	0.0589
wR2[b]	0.1538	0.1025	0.1373
largest diff peak/hole (e Å^{-3})	0.319/−0.282	0.299/−0.223	0.473/−0.231

[a] $R1 = \sum||F_o| - |F_c||/\sum|F_o|$. [b] $wR2 = \{\sum[w(F_o^2 - F_c^2)^2]/[w(F_o^2)^2]\}^{1/2}$.

Table 2. Selected Bond Distances (Å) and Angles (deg) for 1

C(1)−C(7)	1.489(5)	C(15)−C(16)	1.558(5)
C(7)−C(11)	1.340(5)	C(16)−C(17)	1.516(5)
C(11)−C(12)	1.455(6)	C(16)−C(20)	1.519(6)
C(11)−C(15)	1.517(5)	C(17)−C(18)	1.514(6)
C(12)−C(13)	1.328(5)	C(17)−C(27)	1.309(5)
C(13)−C(14)	1.492(5)	C(18)−C(19)	1.508(6)
C(14)−C(15)	1.564(5)	C(19)−C(20)	1.332(6)
C(14)−C(18)	1.567(5)	C(21)−C(27)	1.490(6)
C(1)−C(7)−C(11)	126.9(4)	C(18)−C(19)−C(20)	108.2(4)
C(11)−C(12)−C(13)	111.6(4)	C(16)−C(20)−C(19)	107.3(4)
C(12)−C(13)−C(14)	113.2(4)	C(15)−C(16)−C(17)	98.9(3)
C(14)−C(18)−C(19)	106.4(3)	C(18)−C(17)−C(27)	132.6(4)
C(14)−C(15)−C(16)	102.7(3)	C(16)−C(17)−C(27)	131.0(4)
C(14)−C(18)−C(17)	98.5(3)	C(17)−C(27)−C(21)	126.0(4)
C(17)−C(18)−C(19)	99.9(3)		
C(22)−C(21)−C(27)−C(17)	65.1(6)		
C(2)−C(1)−C(7)−C(11)	69.1(6)		

isomers of *ansa*-calcocene **3** was observed in the ^{1}H NMR spectrum of the crude product formed in THF. A higher *rac*:*meso* ratio of 1.5:1 was observed in the product of the reaction carried out in DME, but the selectivity is still lower than that achieved with 6-phenylfulvene. The ^{1}H and ^{13}C NMR signals for each isomer were assigned through a combination of COSY and HMQC experiments (see Experimental Section). We conclude from our results with the other 6-arylfulvenes that the major product is the *rac* isomer. The ratio of isomers was determined by comparing the intensities of the ^{1}H NMR signals for the methine protons in the ethylene bridge. Due to the high solubility of these calcocenes, isolation of the major isomer by recrystallization was not accomplished.

6-(1-Naphthyl)fulvene. We considered the possibility that the reduced diastereoselectivity of 6-(3,5-di-*tert*-butylphenyl)fulvene coupling relative to 6-phenylfulvene was due to the higher temperature required for the reaction of the bulkier substrate. Therefore, we examined the coupling of 6-(1-naphthyl)fulvene with calcium, since this substrate exhibited higher *rac* selectivity than 6-phenylfulvene when coupled by group 4 transition-metal dihalides.[12] Moreover, we expected this fulvene to react more readily with calcium at room temperature.

Like 6-phenylfulvene, 6-(1-naphthyl)fulvene reacts immediately with activated calcium at room temperature with the evolution of heat to form the *ansa*-calcocene **4**. A ^{1}H NMR spectrum of the crude reaction product showed that the *rac* and *meso* coupling products were present in essentially equal amounts. After redissolving the crude product in DME and refluxing the solution briefly, a white precipitate formed which contained only one of the two isomers. ^{1}H and ^{13}C NMR signals were assigned to each isomer through a combination of COSY and HMQC experiments (see Experimental Section). On the basis of the properties of our other 1,2-diarylethylene-bridged calcocenes, we expect the less soluble isomer to be the *rac* species, but we cannot be certain of this without X-ray crystallographic confirmation.

6-*tert*-Butylfulvene. We expected 6-*tert*-butylfulvene to exhibit high selectivity for the *rac ansa*-calcocene isomer, due to the close proximity of the bulky *tert*-butyl group to the bridge-forming carbon. On the contrary, this substrate produced essentially equal amounts of the *rac* and *meso* coupling products, as determined from integrating a ^{1}H NMR spectrum of the crude product. Whereas the *rac* isomer, *rac*-**5**, crystallizes selectively from a THF solution of the isomer mixture, the *meso* isomer, *meso*-**5**, crystallizes selectively from a DME solution of the isomer mixture. The different solubilities

of the two isomers in these two solvents enabled us to separate and purify each species. The molecular structure of each isomer was determined by X-ray crystallography.

X-ray Crystal Structures of DME Adducts of *rac*- and *meso*-{1,1′-(1,2-*t*-Bu-C_2H_2)(η^5-C_5H_5)}$_2$Ca. Single crystals of *rac*-**5** were initially grown from THF; however, an accurate solution of the molecular structure was prevented by crystal twinning. Therefore, *rac*-**5** was redissolved in DME and single crystals of the DME adduct were grown. Single crystals of *meso*-**5** were also grown from DME. Crystallographic data for the compounds are listed in Table 1. In the structure for *rac*-**5** there were two unique molecules in the unit cell; they are labeled *rac*-**5a** and *rac*-**5b**. Drawings of molecular structures of *rac*-**5a**, *rac*-**5b**, and *meso*-***5*** are shown in Figure 2. Two views of each of the molecules are provided. The ball-and-stick drawings illustrate the conformation of the disubstituted ethylene backbone in each molecule. The ORTEP drawings illustrate top views of each metallocene. Selected bond distances and angles for *rac*-**5a**, *rac*-**5b,** and *meso*-**5** are compared in Table 3.

The most striking feature is the presence of a second molecule of DME on the calcium in the structure of *rac*-**5b**, making the calcium effectively nine-coordinate. This is the first time we have observed this additional ligand coordination in our ethylene-bridged *ansa*-calcocene systems. The structure of $Me_2Si(fluorenyl)_2Ca\cdot 3THF$ reported by Harder et al.[19] is somewhat related; however, the peripheral η^3 coordination of the two fluorenyl rings in this species gives it a lower effective coordination number than that of *rac*-**5b**. The additional DME ligand causes an elongation in the bonds between the calcium and its remaining ligands. The Ca−O bond lengths in *rac*-**5b** are more than 0.1 Å longer than those in *rac*-**5a** and *meso*-**5**. Each of the Ca−ring centroid distances in *rac*-**5b** are also longer than those in *rac*-**5a** and *rac*-**5** by 0.02−0.08 Å. The additional monodentate DME in *rac*-**5b** also causes a slight contraction in the O(1)−Ca−O(2) angle of the chelated DME ligand to 64.69(8)°, as compared with 68.30(9) and 67.19(11)° for *rac*-**5a** and *meso*-**5**, respectively.

Another important feature in each of these structures is the relative disposition of the *tert*-butyl substituents in the ethylene bridge. The drawings of the backbone of each complex in Figure 2d−f illustrate the zigzag arrangement of the ethylene bridge, which sets up axial and equatorial positions for the *tert*-butyl substituents.[20] A diequatorial arrangement of *tert*-butyl groups is preferred for both *rac*-**5a** and *rac*-**5b** as seen from the top views of *rac*-**5a** and *rac*-**5b** in Figure 2a,b. This arrangement distances the *tert*-butyl substituents from nonbonded steric interactions with the cyclopentadienyl rings; however, it also places them in closer proximity to each other, requiring them to adopt a staggered arrangement among their methyl groups. The *cis* disposition of the *tert*-butyl groups in *meso*-**5** requires one *tert*-butyl substituent to be axial, where it is in closer proximity to the cyclopentadienyl ring, as can be seen from the top view of the complex in Figure 2c. The conformation of the backbone lowers the symmetry of the metallocene from C_s to C_1. The lack of symmetry in the frozen-out structure of *meso*-**5** gave us the rare opportunity to use variable-temperature ^{1}H NMR spectroscopy to characterize the rearrangement of the chelating, *ansa*-metallocene ligand framework between right- and left-handed conformations.

Variable-Temperature ^{1}H NMR Characterization of *meso*-5 and *rac*-5. Since the room-temperature ^{1}H NMR spectrum of *meso*-**5** exhibits a broad resonance for the *tert*-butyl substituents, indicative of dynamic behavior, a variable-temperature ^{1}H NMR study was performed. Two different dynamic processes for this compound were identified. One involves restricted rotation of the *tert*-butyl groups of the *ansa* bridge. The other involves a conformational rearrangement of ethylene bridge (and the attached cyclopentadienyl rings) between right and left zigzag orientations, also referred to as δ and λ conformations,[21] as illustrated in Figure 3. Figure 4 shows a series of 500 MHz ^{1}H NMR spectra for *meso*-**5** in THF-d_8 which follow the changes that occur as the sample is cooled from 298 to 180 K. At 298 K the compound exhibits a simple ^{1}H NMR spectrum with only two resonances for the cyclopentadienyl protons at 5.86 ppm (2H) and 5.52 ppm (6H), the latter being a superposition of resonances for three pairs of chemically and magnetically inequivalent protons. There is a single resonance at 3.64 ppm for the methine protons in the bridge and a single resonance at 1.31 ppm for the *tert*-butyl groups. The DME appears as two singlets at 3.43 and 3.27 ppm and is presumably displaced from the calcium center by the THF-d_8 solvent.

The first notable change upon lowering the temperature of the sample was a broadening of the *t*-Bu resonance. At 245 K the resonance became asymmetric, and below 239 K it split into two broad resonances (1.42 and 1.06 ppm) with a 2:1 ratio of intensities. With further cooling, the resonance at 1.06 ppm decoalesced at 232 K ($\Delta G^{\ddagger}_{232} = 11.2 \pm 0.5$ kcal mol^{-1}) to give two broad resonances of equal intensity. These signals sharpened as the sample was cooled to 223 K, and the signal at 1.42 ppm transformed into a sharp resonance overlapping a very broad resonance. The sharp resonance is clearly associated with the two upfield resonances of equal intensity (3H each) at 1.07 and 0.94 ppm at 180 K. These three signals correspond to the methyl groups of one *t*-Bu substituent. The very broad resonance at ca. 1.45 ppm corresponds to the other *t*-Bu group. It decoalesced at 204 K ($\Delta G^{\ddagger}_{204} = 9.2 \pm 0.7$ kcal mol^{-1}) into three, rather broad, resonances at 1.69, 1.47, and 1.23 ppm. The decoalescence of the *tert*-butyl groups into two sets of three inequivalent methyl groups can be attributed to a slowing of the rotation of the *tert*-butyl moieties. That the two *tert*-butyl groups become inequivalent from each other and exhibit different rotational energy barriers is a result of their different environments in the frozen-out form of the complex, as

(19) Harder, S.; Lutz, M.; Straub, A. W. G. *Organometallics* **1997**, *16*, 107−113.

(20) The axial and equatorial descriptors for the disposition of the substituents in the ethylene bridge correspond to the stereochemical nomenclature applied to the chair form of cyclohexane. For additional examples see: (a) Jany, G.; Fawzi, R.; Steimann, M.; Rieger, B. *Organometallics* **1997**, *16*, 544−550. (b) Rieger, B.; Stiemann, M.; Fawzi, R. *Chem. Ber.* **1992**, *125*, 2373−2377. (c) Rieger, B.; Jany, G.; Fawzi, R.; Steimann, M. *Organometallics* **1994**, *13*, 647−653.

(21) See ref 20a, and references therein, for a discussion of the conformations of ethylene-bridged complexes.

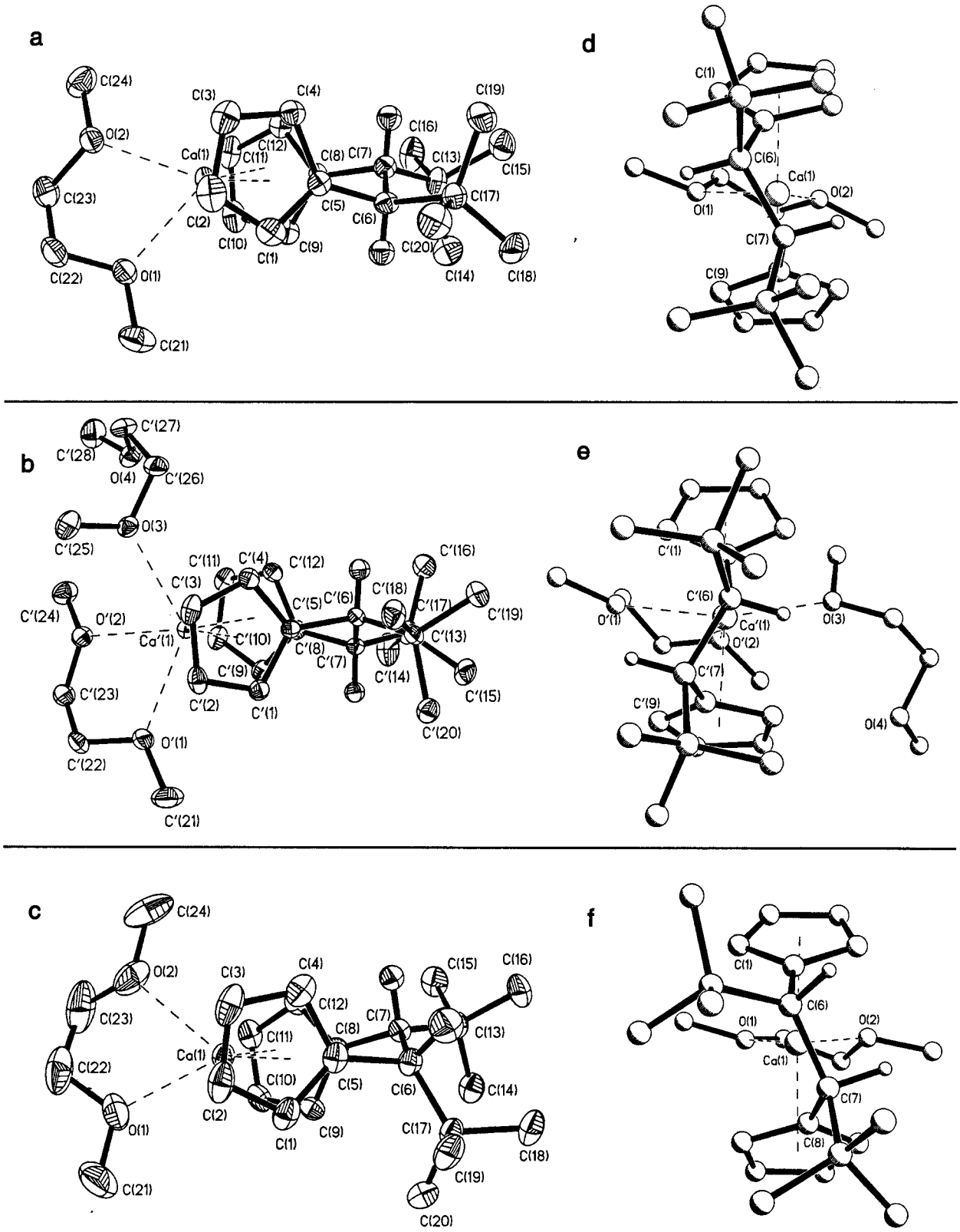

Figure 2. ORTEP drawings (30% ellipsoids) of top views of (a) *rac*-**5a**, (b) *rac*-**5b**, and (c) *meso*-**5** and ball-and-stick drawings of rear views of (d) *rac*-**5a,** (e) *rac*-**5b**, and (c) *meso*-**5**.

seen in the X-ray crystal structure (vide supra). In the frozen-out structure, not only the *tert*-butyl substituents but also the two methine hydrogens in the bridge and all eight hydrogens of the cyclopentadienyl rings become inequivalent. Thus, in the solid state, the compound is not truly *meso*; however, it must pass through a highly symmetric *meso* structure while switching between the two conformations of the backbone. The barrier to this process can be determined by examining the coalescence behavior the signals for the methine protons of the bridge and of the signals for the cyclopentadienyl protons. The signal for the methine protons of the bridge

Table 3. Comparison of Selected Bond Distances and Angles for *trans*-5a, *trans*-5b, and *cis*-5

Bond Distances (Å)

	rac-**5a**	*rac*-**5b**	*meso*-**5**
Ca−Cp(Xa)[a]	2.352(2)	2.429(2)	2.378(4)
Ca−Cp(Xb)[b]	2.357(2)	2.397(2)	2.346(4)
Ca−C(1)	2.665(4)	2.683(3)	2.604(3)
Ca−C(2)	2.673(4)	2.676(3)	2.591(3)
Ca−C(3)	2.641(4)	2.676(3)	2.660(3)
Ca−C(4)	2.599(4)	2.670(3)	2.730(3)
Ca−C(5)	2.628(4)	2.699(4)	2.721(3)
Ca−C(8)	2.641(4)	2.715(3)	2.610(3)
Ca−C(9)	2.640(4)	2.689(3)	2.572(3)
Ca−C(10)	2.660(4)	2.710(3)	2.646(3)
Ca−C(11)	2.646(4)	2.722(4)	2.679(3)
Ca−C(12)	2.628(4)	2.705(4)	2.658(3)
Ca−O(1)	2.410(3)	2.548(3)	2.409(3)
Ca−O(2)	2.432(3)	2.539(3)	2.400(3)
Ca−O(3)		2.517(3)	

Bond Angles (deg)

	trans-**5a**	*trans*-**5b**	*cis*-**5**
Cp(Xa)−Ca−Cp(Xb)	117.47(5)	114.03(4)	119.3(2)
Cp−Cp	61.0(1)	61.9(1)	61.5(2)
O(1)−Ca−O(2)	68.30(9)	64.69(8)	67.19(11)
O(4)−Ca−O(5)		70.94(7)	
Cp−CH−CH−Cp[c]	−46.5(4)	44.5(3)	−40.4(3)
t-Bu−CH−CH−*t*-Bu[d]	59.2(5)	−62.9(4)	−46.3(4)

[a] Xa = centroid of C(1)−C(5) ring. [b] Xb = centroid of C(8)−C(12) ring. [c] C(5)−C(6)-C(7)−C(8). [d] C(17)−C(6)-C(7)−C(13).

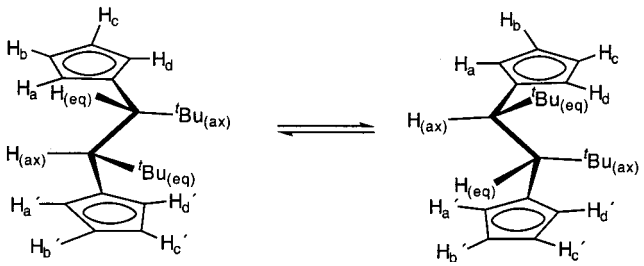

Figure 3. Representation of rearrangement of *meso*-**5** between δ and λ conformations.

broadened and decoalesced at 227 K ($\Delta G^{\ddagger}_{227} = 10.9 \pm 0.5$ kcal mol^{-1}) to give two doublets ($^3J_{HH} = 6.7$ Hz) at 3.63 and 3.51 ppm. The cyclopentadienyl resonance at 5.86 ppm (2H) decoalesced at 232 K ($\Delta G^{\ddagger}_{232} = 11.4 \pm 0.5$ kcal mol^{-1}) to give two multiplets at 5.94 ppm (1H) and 5.71 ppm (1H) at 180 K. The signal at 5.52 ppm due to superimposed cyclopentadienyl resonances (6H) broadened at its base so that two sets of resonances appeared. One set decoalesced at 235 K into two signals which froze out at 5.63 ppm (1H) and 5.30 ppm (1H) at 206 K ($\Delta G^{\ddagger}_{235} = 10.9 \pm 0.5$ kcal mol^{-1}). The other set decoalesced at 226 K into two signals which froze out at 5.59 ppm (1H) and 5.46 ppm (1H) at 206 K ($\Delta G^{\ddagger}_{226} = 10.9 \pm 0.5$ kcal mol^{-1}). The remaining resonance at 5.52 ppm (2H) decoalesced at 206 K into two signals which froze out at 5.53 ppm (1H) and 5.52 ppm (1H) at 180 K. The resonance at 5.86 ppm decoalesced at 232 K ($\Delta G^{\ddagger}_{232} = 10.9 \pm 0.5$ kcal mol^{-1}) to give two multiplets at 5.94 ppm (1H) and 5.71 ppm (1H) at 180 K. The similar values for the free energy of activation calculated at each of these coalescence points supports the involvement of a single fluxional process in averaging the environments of each of these different sets of protons. Line shape analysis of the methine proton signals of the ethylene bridge was performed by modeling the spectra

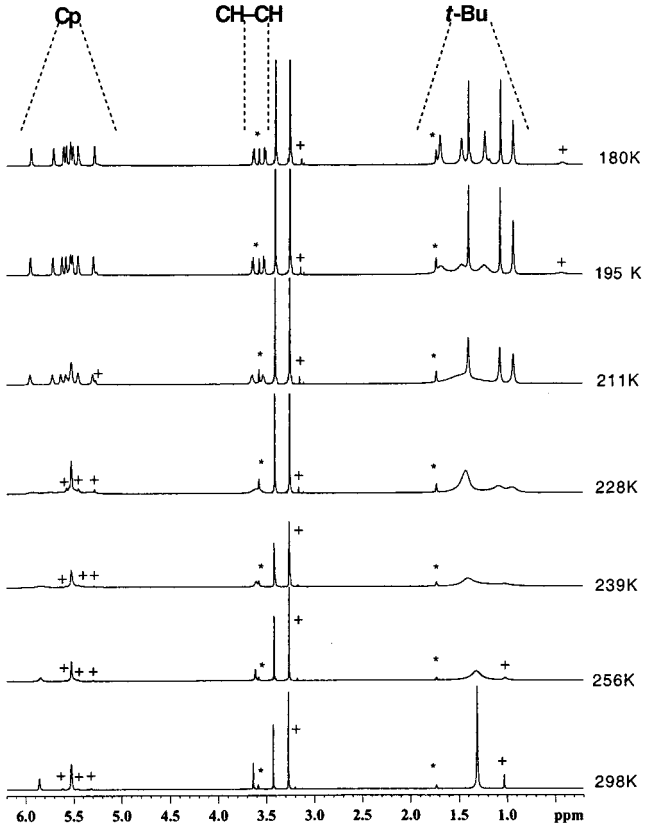

Figure 4. Variable-temperature ^{1}H NMR spectra of *meso*-**5** in THF-d_8 showing decoalescence of resonances for the *t*-Bu groups, bridge methine protons, and cyclopentadienyl ring protons. Resonances due to a small amount of *rac*-**5** isomer impurity are marked with plus signs. Residual proton signals from the solvent are marked with asterisks.

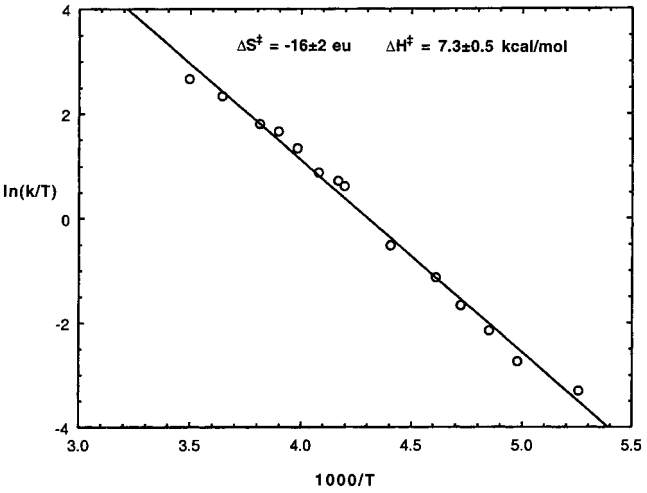

Figure 5. Eyring plot for conformational rearrangement of *meso*-**5**.

with the Spin Works computer software package to obtain the rates for the bridge fluctuation over the temperature range 190−285 K. An Eyring plot of these rates (Figure 5) gave the values $\Delta S^{\ddagger} = -16 \pm 2$ eu and $\Delta H^{\ddagger} = 7.3 \pm 0.5$ kcal mol^{-1} for the conformational rearrangement. The magnitude of $\Delta S^{\ddagger}$ seems large for such a unimolecular rearrangement, in comparison to the $\Delta S^{\ddagger}$ value of −3 eu for the chair-to-chair conformational rearrangement of *cis*-di-*tert*-butylcyclohexane.[22] In fact, the value of $\Delta S^{\ddagger}$ is approaching the values

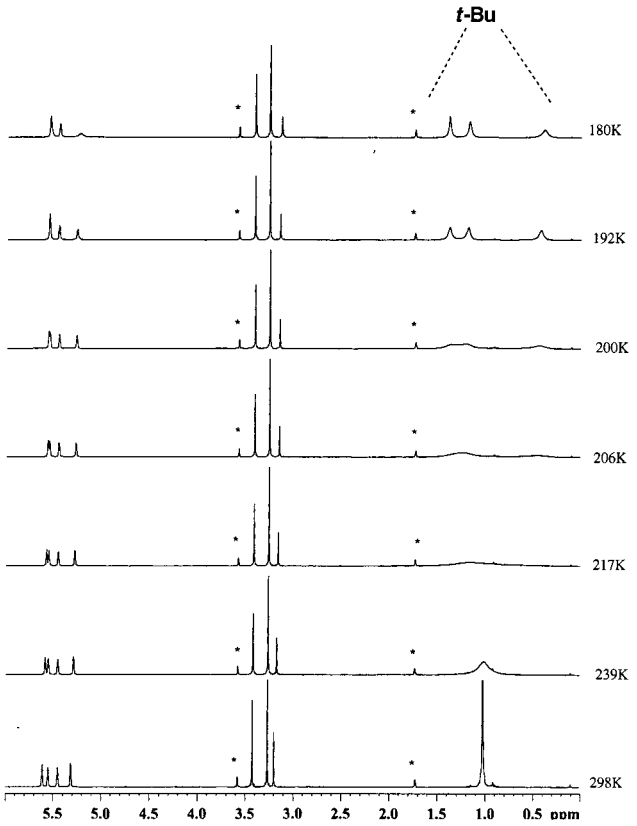

Figure 6. Variable-temperature ^{1}H NMR spectra of *rac*-**5** in THF-d_8 showing decoalescence of the *t*-Bu resonances. Residual proton signals from the solvent are marked with asterisks.

observed for associative intermolecular ligand substitution reactions.[23] This suggests that the THF solvent is playing a role in the rearrangement, possibly through coordination of a third molecule of THF to the calcium. The additional DME coordination seen in *rac*-**5b** (vide supra) offers support for this proposal. Support also comes from the observation that all of the ligand ^{1}H NMR signals for *meso*-**5** are considerably broader in DMSO-d_6 than in THF-d_8. We plan to explore this hypothesis further by measuring the dynamics of the conformational rearrangement of *meso*-**5** in other solvents and by examining the conformational rearrangement of this ligand framework on other metals, such as zirconium and iron.

A variable-temperature ^{1}H NMR study of *rac*-**5** was also undertaken, as shown in Figure 6. The occurrence of any bridge fluctuation is not discernible in this case, since the *tert*-butyl groups would remain in equivalent environments throughout the conformation change. However, the effects of restricted rotation of the *tert*-butyl substituents are observed. At 298 K, a simple spectrum was observed with four pseudo-triplets at 5.61, 5.55, 5.45, and 5.32 ppm for the cyclopentadienyl ring protons, a singlet at 3.20 ppm for the methine protons in the bridge, and a sharp, single resonance at 1.02 ppm for the *tert*-butyl substituents. The singlet for the *t*-Bu groups broadened asymmetrically as the temperature was lowered and split into two broad resonances at 1.25 ppm (12H) and 0.46 ppm (6H) at 217 K. Cooling the sample further to 169 K caused the downfield signal to split into two sharp peaks of equal intensity at 1.39 and 1.18 ppm. The 0.46 ppm peak shifted upfield to 0.39 ppm and became somewhat broadened. From the top views of *rac*-**5a** and *rac*-**5b** shown in Figure 2a,b, it is reasonable to attribute the high-field methyl resonance at 0.39 ppm to the methyl groups oriented toward the bridge (C(16), C(20), C′(14), and C′(18)), since they would be more electronically shielded in this environment. Furthermore, these methyl groups are more crowded than the others, and their restricted rotation would account for the slight broadening of the high-field signal upon cooling the sample from 190 to 169 K. A barrier of $\Delta G^{\ddagger} = 10.2 \pm 0.5$ kcal mol^{-1} at 202 K was estimated for the exchange of environments of the methyl groups pointing away from the bridge from the coalescence of their frozen out resonances at 1.37 and 1.19 ppm. Small changes in cyclopentadiene proton resonances were also observed as the sample was cooled to 169 K. The 5.61 ppm resonance merged with the 5.55 ppm resonance, and the resonance at 5.32 ppm shifted to 5.26 ppm and broadened significantly. The methine protons of the bridge remained unchanged.

Discussion and Conclusion

The ability of fulvenes to take part in Diels−Alder reactions, both as dienes and dienophiles, is well-known.[24] Self-dimerization[15,16] and even trimerization[17] by Diels−Alder cyclization has also been documented. By destabilizing the dipolar resonance form of the fulvene, **II** (Figure 7), electron-withdrawing substituents on the fulvene, such as trifluoromethyl[16] and pentafluorophenyl[25] groups, destabilize the fulvene toward Diels−Alder dimerization. Aryl substituents, on the other hand, generally favor the dipolar form due to the contribution from resonance form **III**. DFT calculations by Tacke et al.[26] showed that a mesityl substituent at carbon 6 is less effective at stabilizing this dipole due to the large dihedral angle of 60.8° it must adopt relative to the cyclopentadiene ring plane in order to minimize steric crowding between the ortho methyl groups of the mesityl substituent and the cyclopentadiene ring. Thus, as we have discovered, 6-mesitylfulvene is more vulnerable toward Diels−Alder dimerization than 6-arylfulvenes that are able to adopt more of a planar conjugation.

Increasing the steric bulk of the substituents at the 6-position of the fulvene, in contrast to our expectations, had an adverse effect on the selectivity of calcium-mediated reductive coupling for the *rac ansa*-calcocene product. This contrasts with the results obtained by Eisch and co-workers, in which the reductive coupling of 6-phenyl-, 6-(1-naphthyl)-, and 6-(9-anthryl)fulvene with group 4 metal dihalides exhibited increasing *rac* selectivity. Furthermore, the stereoselectivity of the calcium-mediated phenylfulvene coupling (*rac*:*meso* = 2.3:1) is *greater* than that of the group 4 metal dihalides

(22) Kessler, H.; Gusowski, V.; Hanack, M. *Tetrahedron Lett.* **1968**, 4665−4670.
(23) Atwood, J. D. *Inorganic and Organometallic Reaction Mechanisms*, 2nd ed.; Wiley-VCH: New York, 1996; p 60.
(24) Nair, V.; Anilkumar, G.; Radhakrishnan, K. V.; Sheela, K. C.; Rath, N. P. *Tetrahedron* **1997**, *51*, 17361−17372 and references therein.
(25) Chang, Y.-C.; Shapiro, P. J. Unreported results.
(26) Tacke, M.; Fox, S.; Cuffe, L.; Dunne, J. P.; Hartl, F.; Mahabiersing, T. *J. Mol. Struct.* **2001**, *559*, 331−339.

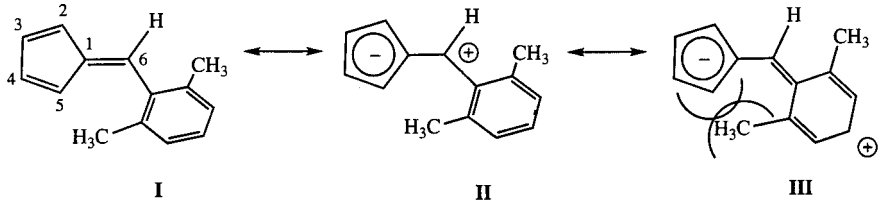

Figure 7. Resonance forms of 6-mesitylfulvene.

(*rac*:*meso* = 1:1). The sensitivity of the stereoselectivity of the homogeneous MCl_2-mediated reaction to the size of the fulvene substituent can be appreciated by invoking a bis(fulvene)metal intermediate similar to that proposed by Tan et al. for the formation of 1,1′-tetramethylethyleneferrocene from 6,6-dimethylfulvene and iron vapor.[27] Strong support for such an intermediate is provided by the bis(η^4-6,6-diphenylfulvene)iron species reported by Teuber et al.,[28] and especially by the bis(η^6-6,6-diphenylfulvene)titanium species reported by Bandy et al.[29] In this arrangement, the substituents on the two fulvenes should have a significant steric influence over the stereochemistry of the bridge formation. On the calcium surface, however, the geometric constraints of the reaction should be quite different, since two fulvene molecules are not able to encapsulate a single metal prior to the coupling step. The coupling must occur either between fulvenes on neighboring calcium atoms or by attack of an external fulvene on an activated, surface-bound fulvene. Since we do not know how the fulvene coupling actually occurs on the calcium surface and how the ligand ultimately chelates an individual metal atom, we cannot explain why the stereoselectivity of the calcium-mediated fulvene coupling is so much better for 6-phenylfulvene than for the other fulvene substrates described herein, especially 6-(1-naphthyl)fulvene. Further experiments are planned to address this question. There are a few examples of fulvenes that have been coupled by calcium and other metals with complete selectivity for the *rac ansa*-metallocene isomer. In these cases inclusion of the exo C=C bond of the fulvene within an annulated ring is key to the stereoselectivity of the coupling.[30−32]

Our ability to capture the dynamic conformational changes in the backbone of the chelating ligand framework of *meso*-**5** on the NMR time scale is due to the barrier imposed on the rearrangement by the bulky *tert*-butyl substituents. In the absence of such bulky substituents, the rearrangements are too fast to be observed on the NMR time scale,[33−35] although Piemontesi,[34] Resconi,[35] and co-workers have been able to determine the equilibrium ratios and thus the energy differences between the λ and δ conformers of *rac* ethylene-bridged bis(indenyl)zirconocene dichloride complexes by analyzing the coupling between the hydrogens on the bridge. The effect of the bridge conformation on the disposition of the indenyl rings over the active site of the metal has been found to influence catalyst stereoselectivity during α-olefin polymerization.[20,34] Therefore, the reductive coupling of asymmetric fulvenes to form *ansa*-metallocenes with bulky substituents in the bridge which offer control over the conformational rearrangement of the bridge should be useful for the design of metallocene ligand frameworks for stereoselective α-olefin polymerization catalysis.

In summary, our survey of bulky 6-aryl- and 6-alkylfulvenes in the synthesis of *ansa*-calcocenes using the Edelmann method revealed that 6-mesitylfulvene cannot be coupled by this method, due to its proclivity for self-dimerization. We also learned that increasing the steric bulk of the substituents on the asymmetrically substituted fulvene can have an adverse affect on the *rac* selectivity of the *ansa*-metallocene formation when heterogeneous reductive coupling methods are used. Finally, we have been able to examine, for the first time, the dynamics of the rearrangement of an ethylene-bridged metallocene complex between λ and δ conformations as a result of the steric barrier imposed by the bulky *tert*-butyl groups on the rearrangement. The role played by the THF solvent in this rearrangement is currently being explored.

Experimental Section

General Considerations. 6-Mesitylfulvene, 6-(3,5-di-*tert*-butylphenyl)fulvene, 6-*tert*-butylfulvene,[13] and 6-(1-naphthyl-fulvene)[12] were prepared by following the method described by Little and Stone.[13] 3,5-Di-*tert*-butylbenzaldehyde was prepared as described in the literature.[36] Calcium chips were activated with $HgCl_2$ as described by Edelmann and co-workers.[7] Tetrahydrofuran, dimethoxyethane, toluene, petroleum ether, and pentane were stored over and distilled from Na/benzophenone immediately prior to use. All other reagents were used as received. Air- and moisture-sensitive compounds were handled and stored in a nitrogen-filled glovebox and were manipulated using argon and vacuum Schlenk techniques. ^{1}H and ^{13}C NMR spectra were recorded on Bruker AC 200 (200 MHz, ^{1}H; 50 MHz, ^{13}C), Bruker AMX 300 (300 MHz, ^{1}H; 75 MHz, ^{13}C), or Bruker AVANCE 500 (500 MHz, ^{1}H; 125 MHz, ^{13}C) spectrometers and referenced to the proton impurity of the solvent (C_6D_6, 7.15; d_6-DMSO, 2.50; d_8-THF, 1.73). Mass spectrometric measurements were obtained on a JEOL JMS-AX505HA spectrometer. Elemental analyses were performed by Desert Analytics (Tuscon, AZ).

Preparation of Mesitylfulvene Monomer and Dimer, 1. Pyrrolidine (5.0 mL, 0.060 mol) was added to a flask

(27) Tan, T. S.; Fletcher, J. L.; McGlinchey, M. J. *J. Chem. Soc., Chem. Commun.* **1975**, 771−772.
(28) Teuber, R.; Köppe, R.; Linti, G.; Tacke, M. *J. Organomet. Chem.* **1997**, *545*−*546*, 105−110.
(29) Bandy, J. A.; Mtetwa, V. S. B.; Prout, K. *J. Chem. Soc., Dalton Trans.* **1985**, 2037−2049.
(30) Fedushkin, I. L.; Dechert, S.; Schumann, H. *Angew. Chem., Int. Ed.* **2001**, *40*, 561−563.
(31) Burger, P.; Hund, H.-U.; Evertz, K.; Brintzinger, H.-H. *J. Organomet. Chem.* **1989**, *378*, 153−161.
(32) Könemann, M.; Erker, G.; Fröhlich, R.; Kotila, S. *Organometallics* **1997**, *16*, 2900−2908.
(33) Collins, S.; Hong, Y.; Taylor, N. J. *Organometallics* **1990**, *9*, 2695−2703.
(34) Piemontesi, F.; Camurati, I.; Resconi, L.; Balboni, D.; Sironi, A.; Moret, M.; Ziegler, R.; Piccolrovazzi, N. *Organometallics* **1995**, *14*, 1256−1266.
(35) Resconi, L.; Piemontesi, F.; Camurati, I.; Balboni, D.; Sironi, A.; Moret, M.; Rychlicki, H.; Ziegler, R. *Organometallics* **1996**, *15*, 5046−5059.
(36) Newman, M. S.; Lee, L. F. *J. Org. Chem.* **1972**, *37*, 4468−4469.

containing a solution of freshly cracked cyclopentadiene (11 mL, 0.13 mol) and mesitaldehyde (5.0 mL, 0.034 mol) and 100 mL of methanol at 0 °C. The reaction mixture turned yellow with the addition of pyrrolidine and became orange within 10 min. After it was stirred for 12 h at room temperature, the dark orange, almost black, reaction mixture was quenched by adding 10 mL of acetic acid and 100 mL of ice. The aqueous/organic mixture was extracted with 4 × 50 mL of petroleum ether. The fulvene product distilled over at 55 °C (20 mTorr). It turned from a clear, glassy material to an opaque crystalline solid, which was primarily the dimer (yield 5.15 g, 77%; mp 128.3−128.7 °C). Monomer: ^{1}H NMR (200 MHz, $CDCl_3$) δ 7.18 (s, 1H, {C_5H_4}C*H*Aryl), 6.90 (s, 2 H, Aryl *H*), 6.49 (m, overlapping signals, 2 H, C_5H_4), 6.33 (m, 1H, C_5H_4), 6.05 (m, 1H, C_5H_4), 2.3 (s, 3H, *p*-CH_3), 2.19 (s, 6H, *o*-CH_3). Dimer ((*E*,*E*)-5,10-bis(mesitylmethylene)tricyclo[5.2.1.0]deca-3,8-diene; protons and carbons are numbered according to the numbering scheme of the molecular structure in Figure 1, and assignments are based on ^{1}H, ^{13}C, COESY, HMQC, and HMBC NMR spectra): ^{1}H NMR (500.13 MHz, $CDCl_3$) δ 6.877 (s, 2H, H3 + H5), 6.859 (s, 2H, H23 + H25), 6.239 (dd, $^3J_{HH}$ = 5.9 Hz, $^4J_{HH}$ = 2.9 Hz, 1H, H12), 6.167 (s, 1H, H27), 6.003 (dd, $^3J_{HH}$ = 5.9 Hz, $^4J_{HH}$ = 2.9 Hz, 1H, H13), 5.830 (dd, J_{HH} = 5.7 Hz, J_{HH} = 0.9 Hz, 1H, H20), 5.782 (m, 1H, H19), 5.618 (s, 1H, H7), 3.577 (pseudo t, J_{HH} = 3.7 Hz, 1H, H15), 3.501 (ddd, $^3J_{HH}$ = 6.7 Hz, $^3J_{HH}$ = 4.8 Hz, $^3J_{HH}$ = 1.9 Hz, 1H, H14), 3.278 (m, 1H, H16), 2.871 (pseudo t, J_{HH} = 3.3 Hz, 1H, H18), 2.302 (s, 3H, *p*-Me9), 2.287 (s, 3H, *p*-Me29), 2.193 (s, 6H, *o*-Me8+10), 2.185 (s, 6H, *o*-Me28+30); ^{13}C NMR (125.76 MHz, $CDCl_3$) δ 158.19 (C11), 148.08 (C17), 138.89 (C19), 136.59 (C1 + C21), 136.20 (C20), 136.16 (C24), 135.62 (C4), 134.41 (C22 + C26), 133.10 (C12), 133.02 (C2 + C6), 132.81 (C13), 127.91 (C23 + C25), 127.79 (C3 + C5), 117.50 (C27), 105.11 (C7), 50.73 (C15), 50.47 (C16), 46.79 (C14), 44.37(C19), 20.94 (C9), 20.93 (C29), 20.63 (C28 + C30), 20.37 (C8 + C10). Anal. Found (calcd) for $C_{15}H_{16}$: C, 91.75 (91.78); H, 8.27 (8.22). Mp (uncorrected): 128.5−128.7 °C. Crystals of the dimer suitable for X-ray analysis were obtained by recrystallization from petroleum ether.

Preparation of 6-(3,5-Di-*tert*-butylphenyl)fulvene (2). The procedure was similar to that described above. The reaction of 3,5-di-*tert*-butylbenzaldehyde (4.0 g, 18 mmol) and cyclopentadiene (4.8 mL, 59 mmol) in the presence of pyrrolidine (2.7 mL, 32 mmol) afforded 5.1 g of a thick, brown oil that contained the fulvene, dicyclopentadiene, and other unidentified impurities. ^{1}H NMR (300 MHz, $CDCl_3$): δ 7.47 (s, 2H, *o*-Aryl H), 7.29 (s, 1H, *p*-Aryl H), 6.71−6.66 (overlapping multiplets, 2H, C_5H_4 and (C_5H_4)C*H*(Aryl)), 6.41 (br d, $^3J_{HH}$ = 5 Hz, 1H, C_5H_4), 6.36 (dt, $^3J_{HH}$, = 5.1 Hz, J_{HH} = 1.7 Hz, 1H, C_5H_4), 5.86 (m, 1H, C_5H_4), 1.35 (s, 18H, C(CH_3)$_3$). MS (EI): *m*/*z* 266 (M^+, 100.0), 251 ($M^+ - CH_3$, 54.0), 236 ($M^+ - (2 \times CH_3)$, 19.6), 221 ($M^+ - (3 \times CH_3)$, 40.0), 209 ($M^+ - C(CH_3)_3$, 84.6), 195.

Preparation of {(1,1′-[1,2-(3,5-(^{t}Bu)$_2$-C$_6$H$_3$)$_2$C$_6$H$_3$)C$_2$H$_2$]-(η^5-C$_5$H$_4$)$_2$}Ca·DME (3). The reaction was carried out as described above, but in dimethoxyethane. The fulvene (10.0 g, 38 mmol) was reacted with activated calcium (980 mg, 24 mmol). The crude reaction product, a brown oil, showed two isomers in a ratio of 1.5:1. Washing the oil with pentane afforded a beige powder (yield: 4.7 g, 37% based on fulvene). The beige powder contained a similar ratio of the two isomers (based on the ratio of the bridge protons). ^{1}H NMR (500 MHz, DMSO-d_6): δ 7.01 (d, 2H, *o*-Aryl *H*, either isomer), 6.98 (br, 2H, *o*-Aryl *H*, either isomer), 6.94 (t, 1H, *p*-Aryl *H*, major isomer), 6.84 (t,1H, p-Aryl *H*, minor isomer) 5.96 (m, 1H, C_5H_4, minor), 5.79 (2 overlapping m, 2H, C_5H_4, major), 5.59 (2 overlapping m, 2H, both isomers), 5.53 (m, 1H, C_5H_4, minor), 5.48 (m, 1H, C_5H_4, major), 5.36 (m, 1H, C_5H_4, minor), 4.74 (s, C*H*-Aryl, major), 4.42 (s, C*H*-Aryl, minor), 3.42 (s, 4H, DME), 3.24 (s, 6H, DME), 1.14 (s, 18H, *t*-Bu, both isomers). ^{13}C NMR (DMSO-d_6): δ 148.2, 147.7, 146.2, 142.8 (*o*- and *p*-Aryl *C*, both isomers), 122.6, 122.3, 124.2, 124.0, 117.4, 117.2 (*m*-Aryl *C*, ipso-Aryl *C*, and ipso-C_5H_4, both isomers), 107.7, 107.5, 105.6, 104.8 (C_5H_4, major), 107.0, 105.9, 103.4, 101.7 (C_5H_4, minor), 71.1, 58.0 (DME), 56.4, 55.7 (*C*H-*t*-Bu, both isomers), 34.2 ($C(CH_3)_3$, both isomers) 31.4 (C(CH_3)$_3$, both isomers). Since it was not possible to isolate the calcocene free of impurities by recrystallization, an elemental analysis was not obtained. NMR spectra are included in the Supporting Information.

Preparation of {1,1′-[1,2-(C$_{10}$H$_9$)$_2$C$_2$H$_2$](η^5-C$_5$H$_4$)$_2$}Ca·DME (4). An 11.61 g portion of fulvene (76% purity, 43.2 mmol; the 24% impurity was dicyclopentadiene remaining from the fulvene preparation) was added to a suspension of 3.67 g (91.6 mmol) of activated calcium in 150 mL of THF. The orange-red mixture became warm and turned turbid yellow within 15 min. The reaction was stirred at room temperature overnight. The resulting beige mixture was filtered, and the light brown filtrate was dried to a foam under vacuum. After it was dried for an additional 2 h at 70 °C under vacuum, the foam was washed with 2 × 10 mL of pentane. Drying under vacuum gave a cream-colored powder (yield 7.1 g, 55%, based on fulvene). A 50:50 mixture of the *rac* and *meso ansa*-calcocene products was established from the integrations of the ^{1}H signals of the methine protons in the bridge and the protons on the naphthyl rings in a THF-d_8 sample. A 6.01 g portion of the calcocene mixture was completely dissolved in 35 mL of DME. The solid dissolved completely, but after the solution was refluxed for a few minutes it became turbid, and a white precipitate formed. The precipitated material (0.71 g) was a single isomer. The stereochemistry of this less DME soluble isomer has not yet been determined. Its NMR spectral data are as follows. ^{1}H NMR (500.13 MHz, THF-d_8): δ 8.92 (d, $^3J_{HH}$ = 8.54 Hz, 2H, naphthyl), 7.85 (d, $^3J_{HH}$ = 7.42 Hz, 2H, naphthyl), 7.61 (d, $^3J_{HH}$ = 8.54 Hz, 2H, naphthyl), 7.50 (dt, $^3J_{HH}$ = 8.54 Hz, $^4J_{HH}$ = 1.26 Hz, 2H, naphthyl), 7.32 (m, 4H, naphthyl), 7.04 (t, $^3J_{HH}$ = 7.73 Hz, 2H, naphthyl), 6.26 (s, 2H, C*H*-Aryl), 6.18 (pseudo-t, J_{HH} = 2.5 Hz 2H, C_5H_4), 6.00 (pseudo-t, J_{HH} = 2.5 Hz, 2H, C_5H_4), 5.67 (pseudo-t, J_{HH} = 2.5 Hz, 2H, C_5H_4), 5.50 (pseudo-t, J_{HH} = 2.5 Hz, 2H, C_5H_4), 3.44 (s, 4H, DME), 3.28 (s, 6H, DME). ^{13}C NMR (125.76 MHz, THF-d_8): δ 144.66 (C-ipso, Cp), 134.91 (C_{quart} naphthyl), 133.10 (C_{quart}, naphthyl), 129.48 (C_{quart}, naphthyl), 129.16 (*C*H, naphthyl), 126.14 (*C*H, naphthyl), 125.54 (*C*H, naphthyl), 125.41 (*C*H, naphthyl), 125.04 (2 overlapping *C*H, naphthyl), 123.50 (*C*H, naphthyl), 109.03 (*C*H, Cp), 108.62 (*C*H, Cp), 104.78 (*C*H, Cp), 104.76 (*C*H, Cp), 72.71 (CH_2, DME), 58.86 (CH_3, DME), 46.99 (*C*H, bridge).

The NMR data of the more DME soluble isomer are as follows. ^{1}H NMR (500.13 MHz, THF-d_8): δ 8.32 (d, $^3J_{HH}$ = 8.49 Hz, 2H, naphthyl), 8.15 (d, $^3J_{HH}$ = 7.31 Hz, 2H, naphthyl), 7.60 (d, $^3J_{HH}$ = 6.44 Hz, 2H, naphthyl), 7.44 (d, $^3J_{HH}$ = 8.22 Hz, 2H, naphthyl), 7.27−7.18 (overlapping, 6H, naphthyl), 6.37 (s, 2H, C*H*-Aryl), 6.07 (pseudo-t, J_{HH} = 2.3 Hz, 2H, C_5H_4), 5.80 (m, 4H, 2 overlapping C_5H_4), 5.65 (pseudo-t, J_{HH} = 2.3 Hz, 2H, C_5H_4), 3.44 (s, 4H, DME), 3.28 (s, 6H, DME). ^{13}C{^{1}H} NMR (125.76 MHz, THF-d_8): δ 141.30 (C-ipso, Cp), 134.85 (C_{quart}, naphthyl), 133.91 (C_{quart}, naphthyl), 129.68 (*C*H, naphthyl), 129.52 (C_{quart}, naphthyl), 129.01 (CH, naphthyl), 125.80 (*C*H, naphthyl), 125.05 (2 overlapping *C*H, naphthyl), 124.97 (*C*H, naphthyl), 124.86 (*C*H, naphthyl), 109.53 (*C*H, Cp), 108.81 (*C*H, Cp), 107.28 (*C*H, Cp), 106.80 (*C*H, Cp), 72.71 (CH_2, DME), 58.86 (CH_3, DME), 50.37 (*C*H, bridge). Anal. Found (calcd) for $C_{36}H_{34}CaO_2$: C, 80.17 (80.26); H, 6.35 (6.36).

Preparation of *meso*-{1,1′-[1,2-(^{t}Bu)$_2$C$_2$H$_2$](η^5-C$_5$H$_4$)$_2$}-Ca·DME (*meso*-5). A 7.0 g portion (52 mmol) of 6-*tert*-butylfulvene was added to a suspension of 2.25 g (56.2 mmol) of activated calcium in 70 mL of DME. The mixture was heated to reflux and stirred for 4−5 h. The calcium was allowed to settle overnight. The mixture was filtered, and a light orange solution was obtained. Upon being concentrated to half of its original volume under vacuum and cooled at −30 °C, the solution afforded cream-colored crystals which were isolated by filtration (yield 3.3 g, 32% based on fulvene). A ^{1}H NMR

spectrum of the product revealed a 3.3:1 mixture of *meso* and *rac* isomers. A second crop of product (yield 4.7 g, 46%) contained a 1:1 mixture of isomers. The first crop was recrystallized from DME to give material containing 92% *meso* product. The remaining 8% of material was the *rac* isomer. NMR data for *meso*-**5** are as follows. ^{1}H NMR (500.13 MHz, 298 K, THF-d_8): δ 5.86 (m, 2H, C_5H_4), 5.53 (two overlapping m, 6H, C_5H_4), 3.64 (s, 2H, $-C_2H_2-$), 3.43 (s, 4H, DME), 3.27 (s, 6H, DME), 1.31 (s, 18H, 2 × C(CH_3)$_3$). ^{1}H-coupled ^{13}C NMR (125.75 MHz, THF-d_8, 60 °C): δ 128.85 (s, *ipso*-C_5H_4), 111.92 (d, $^1J_{CH}$ = 157.6 Hz, C_5H_4), 108.77 (d, $^1J_{CH}$ = 158.7 Hz, C_5H_4), 105.03 (d, $^1J_{CH}$ = 159.3 Hz, C_5H_4), 104.98 (d, $^1J_{CH}$ = 159.4 Hz, C_5H_4), 72.67 (t, $^1J_{CH}$ = 140.1 Hz, CH_2, DME), 60.63 (d, $^1J_{CH}$ = 122.0 Hz, *C*H, bridge), 58.77 (q, $^1J_{CH}$ = 143.4 Hz, CH_3, DME), 35.71 (s, $C(CH_3)_3$), 33.38 (q, $^1J_{CH}$ = 124.2 Hz, C(CH_3)$_3$). Anal. Found (calcd) for $C_{24}H_{38}CaO_2$: C, 72.05 (72.31); H, 9.59 (9.61).

Preparation of *rac*-{1,1′-[1,2-(^{t}Bu)$_2$C$_2$H$_2$](η^5-C$_5$H$_4$)$_2$}Ca·DME (*rac*-5). A 7.6 g portion (56.6 mmol) of 6-*tert*-butylfulvene was added to 2.48 g (61.9 mmol) of activated calcium in 100 mL of THF. The reaction mixture was heated to reflux and stirred overnight. After it was cooled and allowed to stand for 24 h, the mixture was filtered and the THF was removed under vacuum to afford a brown foam. The foam was washed twice with 100 mL of pentane, giving a beige powder. The product was dissolved in 60 mL of THF, and the solution was cooled to −60 °C to afford 7.43 g of crystalline product (16.4 mmol, 58%). A ^{1}H NMR spectrum of the product showed a 3:1 mixture of *rac* and *meso* isomers. This crop was recrystallized from THF to yield 2.10 g of >95% pure *rac* material. A 1.0 g portion of this material was dissolved in 10 mL of DME, and the solution was refluxed briefly. Slow cooling of the solution afforded small plates of *rac*-**5**, which were used for X-ray analysis. ^{1}H NMR (500.13 MHz, 298 K, THF-d_8): δ 5.61 (pseudo-t, J_{HH} = 2.5 Hz, 2H, C_5H_4), 5.55 (pseudo-t, J_{HH} = 2.5 Hz, 2H, C_5H_4), 5.45 (pseudo-t, J_{HH} = 2.5 Hz, 2H, C_5H_4), 5.32 (pseudo-t, J_{HH} = 2.5 Hz, 2H, C_5H_4), 3.43 (s, 4H, DME), 3.27 (s, 6H, DME), 3.20 (s, 2H, C_2H_2), 1.02 (s, 18H, 2 × C(CH_3)$_3$). ^{1}H-coupled ^{13}C NMR (125.75 MHz, THF-d$_8$, 25 °C): δ 132.95 (s, *ipso*-C_5H_4), 110.43 (d, $^1J_{CH}$ = 158.4 Hz, C_5H_4), 106.31 (d, $^1J_{CH}$ = 159.3 Hz, C_5H_4), 104.74 (d, $^1J_{CH}$ = 160.3 Hz, C_5H_4), 103.50 (d, $^1J_{CH}$ = 159.8 Hz, C_5H_4), 72.58 (t, $^1J_{CH}$ = 139.8 Hz, CH_2, DME), 58.82 (q, $^1J_{CH}$ = 140.0 Hz, CH_3, DME), 55.14 (d, $^1J_{CH}$ = 124.8 Hz, *C*H, bridge), 35.42 (s, $C(CH_3)_3$), 31.82 (q, $^1J_{CH}$ = 123.8 Hz, C(CH_3)$_3$). Anal. Found (calcd) for $C_{24}H_{38}CaO_2$: C, 72.07 (72.31); H, 9.71 (9.61). Although the crystals used for X-ray analysis showed the presence of additional DME in *rac*-**5b**, the additional DME is labile under vacuum and the sample used for elemental analysis contained only one molecule of DME per calcium, as verified by its ^{1}H NMR spectrum.

X-ray Structure Determinations. Crystals of each compound from the syntheses described above were covered in a layer of hydrocarbon oil to protect them from the air. From each batch, a suitable crystal was selected, attached to a glass fiber using silicon grease, and placed in the low-temperature nitrogen stream. Data were collected at 213(2) K for **1** and at 203(2) K for *rac*-**5** and *meso*-**5** using a Siemens SMART 1K instrument (Mo Kα radiation, λ = 0.710 73 Å) equipped with a Siemens LT-2A low-temperature device. The SHELXTL version 5.10 program package was used for structure solution and refinement.[37] Absorption corrections were applied using SADABS.[38]All non-hydrogen atoms were refined anisotropically. Hydrogen atoms were placed geometrically and refined with a riding model. The hydrogen atoms H6 and H7 in *meso*-**5** were located on the difference map and refined to verify the absolute stereochemistry of the bridge. Data were collected to a 2θ value of 50 °C for *rac*- and *meso*-**5**. Data were limited to 2θ = 46.6° for compound **1**, as the diffraction was extremely weak above this limit. Details of the data collection and refinement are given in Table 1. Further details are provided in the Supporting Information.

Analysis of Activation Parameters using Variable-Temperature ^{1}H NMR Spectra. A methanol standard was used to calibrate the temperature of the NMR spectrometer. $\Delta G^‡$ values at coalescence temperatures were calculated using standard equations.[39] The error assigned to these values was based on an estimated ±3 degree error in the temperature. Rates from the variable-temperature spectra of the bridge methine signals were obtained by visually comparing experimental spectra with computed trial line shapes calculated with the Spin Works software package (freeware available by anonymous ftp from pauli.chem.umanitoba.ca in the pub/marat/Spin Works directory). Error analyses for $\Delta H^‡$ and $\Delta S^‡$ were based on Girolami's[40] derivation of $\sigma\Delta H^‡$ and $\sigma\Delta S^‡$ assuming a 10% error in k and a maximum 1.7% error in temperature.

Acknowledgment. We are grateful to the donors of the Petroleum Research Fund, administered by the American Chemical Society, the National Science Foundation (Grant No. CHE-9816730), and the Department of Energy EPSCoR program (Grant No. DE-FG02-98ER45709) for their generous financial support. The establishment of a Single-Crystal X-ray Diffraction Laboratory and the purchase of a 500 MHz NMR spectrometer were supported by the M. J. Murdock Charitable Trust of Vancouver, WA, the National Science Foundations, and the NSF-Idaho EPSCoR Program. We also thank Prof. R. V. Williams for helpful discussions, one of the reviewers of this paper for useful comments, and Prof. G. S. Girolami for helpful advice concerning the evaluation of error in the activation parameter determinations.

Supporting Information Available: Figures giving NMR spectra for **3** (^{1}H, ^{13}C{^{1}H}, COSY, and HMQC) and details of the structure determinations for compounds **1**, *rac*-**5**, and *meso*-**5**, including ORTEP drawings and listings of atomic coordinates, thermal parameters, and bond distances and angles. This material is available free of charge via the Internet at http://pubs.acs.org.

OM010614S

(37) SHELXTL Version 5.10 PCNT; Bruker AXS Inc., Madison, WI, 1999.
(38) SADABS (Bruker/Siemens area detector absorption correction program), an empirical absorption program by G. M. Sheldrick, Bruker AXS Inc., Madison, WI, 1999.
(39) Friebolin, H. *Basic One- and Two-Dimensional NMR Spectroscopy*, 3rd ed.; Wiley-VCH: Weinheim, Germany, 1998; pp 307−308.
(40) Morse, P. M.; Spencer, M. D.; Wilson, S. R.; Girolami, G. S. *Organometallics* **1994**, *13*, 1646−1655.